Multidisciplinary Integrated Framework for the Optimal Design of a Jet Aircraft Wing

Near Optimal Detection of Quantized Signals and Application to JPEG Forensics

Tiziano Bianchi [1], Alessandro Piva [2], Fernando Pérez-González [3]

[1] *Dept. of Electronics and Telecommunications, Politecnico di Torino, Corso Duca degli Abruzzi, 24 - 10129 Torino, Italy*
tiziano.bianchi@polito.it

[2] *Dept. of Information Engineering, University of Florence, Via Santa Marta, 3 - 50139 Firenze, Italy*
alessandro.piva@unifi.it

[3] *Signal Theory and Communications Department, University of Vigo, Campus Universitario - 36310 Vigo, Spain*
fperez@gts.uvigo.es

***Abstract*—In this paper, we investigate the problem of deciding whether a multidimensional signal has been quantized according to a given lattice or not. Under an infinite variance assumption, we derive the expression of the optimal detector, together with a practical approximation formula based on multidimensional Fourier series. As a forensic case study, the proposed detector is applied to the detection of nonaligned double JPEG compression. Results on both synthetic signals and real JPEG images show interesting properties of the proposed detector. Namely, the detector outperforms existing state-of-art detectors for nonaligned double JPEG compression. The application of the proposed scheme to other forensic problems seems a natural extension of this work.**

I. Introduction

Image forensics is a new research area aiming at detecting clues regarding the history of a digital image, by looking for distinctive patterns in statistical and geometrical features, including JPEG quantization artifacts, interpolation, demosaicing traces [1]. An advantage of this approach is that it is passive, in the sense that it is not necessary to embed an explicit fingerprint in the digital image after its acquisition, so that forensics tools can be applied to generic digital images.

Since a vast amount of digital images are currently available in JPEG format, several forensics tools have been developed to detect the presence of specific features in this class of images. A very distinctive feature in digital images is the presence of artifacts due to a previous JPEG compression. In [2], the authors propose a method to determine whether a bitmap image has been previosly JPEG compressed and to estimate the JPEG quantization steps.

Revealing the presence of a previous JPEG compression after JPEG recompression is in general a more difficult task. When the discrete cosine transform (DCT) grids of successive JPEG compressions are perfectly aligned, double JPEG compression can be detected by recompressing the image at different quality levels [3], or by analyzing the statistics of DCT coefficients [4], [5]. In [6], the statistical distribution of first digits in quantized DCT coefficients is successfully used for detecting double JPEG compression. Recent results demonstrate that first digit features can be also used to detect multiple JPEG recompressions [7]. When the discrete cosine transform (DCT) grids of successive JPEG compressions are not aligned, the above methods usually fail. In this case, double JPEG compression can be revealed by considering blocking artifacts [8], or by evaluating the integer periodicity of DCT coefficients when different shifts are applied to the examined image [9]. A very challenging case occurs when some processing has been applied between the two JPEG compressions: in [10], the authors propose a solution for the case of image resizing applied before the second compression.

All of the above approaches consider specific features arising in particular cases. Moreover, there is no guarantee that the chosen features achieve some optimality regarding the detection problem. In [9], [10], it is argued that a previous JPEG compression can be detected by verifying whether DCT coefficients are approximately distributed according to a given quantization lattice, however no optimal detector was proposed for this kind of signals. In this paper, we propose a near optimal detector according to the Neyman-Pearson lemma for signals quantized on a given lattice, where the detector is indeed optimal under an infinite variance assumption. The detection strategy is inspired by the work in [11] regarding the performance of quantization based data hiding algorithms. Since the optimal detector is expressed as an infinite series, several approximate expressions for its practical evaluation are derived and tested on synthetic signals. We also show how to employ the proposed detector in a practical forensic problem, i.e., the detection of double JPEG compression when the DCT grids of the two JPEG compressions are not aligned.

II. Mathematical modeling

We consider a multidimensional signal $\mathbf{x} \in \mathbb{R}^N$, whose probability density function (pdf) depends on the hypotheses $\mathcal{H}_0$: signal is not quantized, and $\mathcal{H}_1$: signal is quantized on a given lattice. We define the probability of detection as the probability of accepting the hypothesis $\mathcal{H}_1$ when $\mathcal{H}_1$ is

WIFS'2013, November 18-21, 2013, Guangzhou, China.
ISBN 978-1-4673-5593-3

true, and the probability of false alarm as the probability of accepting $\mathcal{H}_1$ when $\mathcal{H}_1$ is false. The Neyman-Pearson (NP) lemma states that, given a fixed probability of false alarm, the probability of detection is maximized by the following binary test:

$$\frac{p(\mathbf{x}|\mathcal{H}_1)}{p(\mathbf{x}|\mathcal{H}_0)} \gtrless \tau \tag{1}$$

where $p(\mathbf{x}|\mathcal{H}_0)$ and $p(\mathbf{x}|\mathcal{H}_1)$ are the probability distributions of the signal $\mathbf{x}$ under hypotheses $\mathcal{H}_0$ and $\mathcal{H}_1$, respectively.

We will assume that under hypothesis $\mathcal{H}_1$ the signal is quantized to the points of a lattice defined by the generator matrix $\mathbf{\Theta}$ and perturbed by an additive Gaussian noise vector with covariance matrix $\mathbf{C}$. Its pdf can be derived as

$$p(\mathbf{x}|\mathcal{H}_1) = \sum_{\mathbf{k}\in\mathbb{Z}^N} w(\mathbf{k}) g(\mathbf{x}-\mathbf{\Theta}\mathbf{k};\mathbf{C}) \tag{2}$$

where $g(\mathbf{x};\mathbf{C}) \triangleq |2\pi\mathbf{C}|^{-\frac{1}{2}} e^{-\frac{\mathbf{x}^T\mathbf{C}^{-1}\mathbf{x}}{2}}$ and $\sum_{\mathbf{k}\in\mathbb{Z}^N} w(\mathbf{k}) = 1$. The weights $w(\mathbf{k})$ denote the probability of $\mathbf{x}$ falling within the $\mathbf{k}$th quantization bin. In the following, we will assume that $\mathbf{\Theta}$ is full rank and that $\det(\mathbf{\Theta}) > 0$, so that the volume of the fundamental parallelotope of the lattice is given by $\det(\mathbf{\Theta}) \triangleq |\mathbf{\Theta}|$.

Moreover, we will assume that under $\mathcal{H}_0$ the signal $\mathbf{x}$ is uniformly distributed within the fundamental parallelotope of the lattice: this is usually referred to as the high SNR assumption and is justified if we assume that $\mathbf{\Theta}$ is reduced so that the parallelotope is nearly orthogonal. The resulting pdf can be expressed as

$$p(\mathbf{x}|\mathcal{H}_0) \approx \sum_{\mathbf{k}\in\mathbb{Z}^N} w(\mathbf{k}) \frac{I(\mathbf{\Theta}^{-1}\mathbf{x}-\mathbf{k})}{|\mathbf{\Theta}|} \tag{3}$$

where $I(\mathbf{x}) = 1$ if $||\mathbf{x}||_\infty \leq \frac{1}{2}$, otherwise $I(\mathbf{x}) = 0$.

It is useful to define some quantities for measuring the effect of lattice quantization on a generic signal. According to the familiar concept of signal-to-noise ratio (SNR), we will define the signal-to-lattice ratio (SLR) as the ratio between the average signal power, denoted by σ_x^2 and the power of a noise that is uniformly distributed on the lattice fundamental parallelotope, i.e.,

$$\mathrm{SLR} = 10\log_{10}\frac{N\sigma_x^2}{\mathrm{Tr}\{\mathbf{\Theta}\mathbf{\Theta}^T\}/12}. \tag{4}$$

In a similar way, we can define the lattice-to-noise ratio (LNR) as the ratio between the power of the lattice noise and the average power of the additive Gaussian noise, i.e.,

$$\mathrm{LNR} = 10\log_{10}\frac{\mathrm{Tr}\{\mathbf{\Theta}\mathbf{\Theta}^T\}/12}{\mathrm{Tr}\{\mathbf{C}\}}. \tag{5}$$

It is easy to check that the standard SNR can be obtained as $\mathrm{SNR} = \mathrm{SLR} + \mathrm{LNR}$.

Let us find $\mathbf{k}_\mathbf{x} \in \mathbb{Z}^N$ so that $I(\mathbf{\Theta}^{-1}\mathbf{x} - \mathbf{k}_\mathbf{x}) = 1$. Then we have

$$\frac{p(\mathbf{x}|\mathcal{H}_1)}{p(\mathbf{x}|\mathcal{H}_0)} = \frac{|\mathbf{\Theta}|}{w(\mathbf{k}_\mathbf{x})} \sum_{\mathbf{k}\in\mathbb{Z}^N} w(\mathbf{k}) g(\mathbf{x}-\mathbf{\Theta}\mathbf{k};\mathbf{C}). \tag{6}$$

Under the assumption that the variance of the content is much larger than the power of both the quantization noise and the additive Gaussian noise, i.e., we are both in a very high SLR regime and in a very high SNR regime – sometimes this is referred to as "infinite" variance assumption –, we can approximate the above likelihood ratio as

$$\frac{p(\mathbf{x}|\mathcal{H}_1)}{p(\mathbf{x}|\mathcal{H}_0)} \approx |\mathbf{\Theta}| \sum_{\mathbf{k}\in\mathbb{Z}^N} g(\mathbf{x}-\mathbf{\Theta}\mathbf{k};\mathbf{C}) \triangleq \mathcal{L}(\mathbf{x};\mathbf{\Theta},\mathbf{C}). \tag{7}$$

The above equation is justified by the fact that for high SNR only values of $\mathbf{k}$ close to $\mathbf{k}_x$ will significantly contribute to the shape of $p(\mathbf{x}|\mathcal{H}_1)$, since $g(\mathbf{x};\mathbf{C})$ decays exponentially fast, while for high SLR $w(\mathbf{k})$ will be approximately constant on those values. Hence, under the high SNR–high SLR assumption the optimal NP test becomes:

$$\mathcal{L}(\mathbf{x};\mathbf{\Theta},\mathbf{C}) \gtrless \tau. \tag{8}$$

In order to get a manageable expression for $\mathcal{L}(\mathbf{x};\mathbf{\Theta},\mathbf{C})$, we can observe that it is a periodic function closely resembling the multidimensional Fourier transform of a signal sampled on lattice points [11]. By using multidimensional Fourier expansion over the lattice $\mathbf{\Theta}$ [12, Ch. 12], the likelihood ratio can be expressed as

$$\mathcal{L}(\mathbf{x};\mathbf{\Theta},\mathbf{C}) = \sum_{\mathbf{n}\in\mathbb{Z}^N} \gamma(\mathbf{n}) \cos(2\pi\mathbf{x}^T\mathbf{\Theta}^{-T}\mathbf{n}) \tag{9}$$

where $\gamma(\mathbf{n}) \triangleq \exp(-2\pi^2\mathbf{n}^T\mathbf{\Psi}^{-1}\mathbf{n})$ and $\mathbf{\Psi} = \mathbf{\Theta}^T\mathbf{C}^{-1}\mathbf{\Theta}$. In practice, in the evaluation of (9) we can neglect all terms such that $\gamma(\mathbf{n}) < \epsilon$. For low LNR values, considering only a few terms in (9) is expected to produce a good approximation of $\mathcal{L}(\mathbf{x};\mathbf{\Theta},\mathbf{C})$.

The evaluation of (9) is much more simple if $\mathbf{\Psi}$ is a diagonal matrix, since we can get a separable expression. Let us define $\mathbf{z} = \mathbf{\Theta}^{-1}\mathbf{x}$. Then, we can rewrite (9) as

$$\mathcal{L}(\mathbf{x};\mathbf{\Theta},\mathbf{C}) = \prod_{i=1}^{N}\left[1 + 2\sum_{n_i=1}^{\infty}\exp\left(-2\pi^2\frac{n_i^2}{\psi_i}\right)\cos(2\pi z_i n_i)\right] \tag{10}$$

where ψ_i is the ith diagonal element of $\mathbf{\Psi}$ and n_i, z_i denote the ith component of $\mathbf{n}$, $\mathbf{z}$, respectively. Again, for a practical evaluation of (10) we can neglect all terms such that $\exp(-2\pi^2 n_i^2/\psi_i) < \epsilon$. We will refer to the above detector as the *separable detector*.

Finnaly, under the hypothesis that we have a small perturbed lattice, i.e., we are in a high LNR regime, the following approximation is also possible

$$\mathcal{L}(\mathbf{x};\mathbf{\Theta},\mathbf{C}) \approx |\mathbf{\Theta}| g(\mathbf{x}-\mathbf{\Theta}\mathbf{k}_\mathbf{x};\mathbf{C}). \tag{11}$$

By taking the logarithm, the resulting approximate NP test can be expressed as

$$\frac{\mathbf{e}_\mathbf{x}{}^T\mathbf{C}^{-1}\mathbf{e}_\mathbf{x}}{2} \gtrless \tau' \tag{12}$$

where $\mathbf{e}_\mathbf{x} = (\mathbf{x}-\mathbf{\Theta}\mathbf{k}_\mathbf{x})$ is the distance of $\mathbf{x}$ from the closest lattice point and $\tau' = \log\tau - \log|\mathbf{\Theta}| + \frac{1}{2}\log|2\pi\mathbf{C}|$. The detector based on the above test will be referred to as *distance*

detector. From (11), it is evident that the distance detector tends to become optimal under a high LNR assumption.

III. Application to Doubly Compressed JPEG Images

In this section, we will show how to apply the model described in the previous section for the detection of a double JPEG compression when the DCT grids of the two compressions are not aligned.

A. Evaluation of $\mathbf{\Theta}$ and $\mathbf{C}$

Let us assume that an original 8×8 image block $\mathbf{y}_1$ is JPEG compressed with a quality factor QF_2, and then decompressed. A generic 8×8 image block $\mathbf{y}_2$ can be modeled as follows:

$$\mathbf{y}_2 = \mathbf{D}^{-1}\mathcal{Q}_2(\mathbf{D}\mathbf{y}_1) + \mathbf{E}_2 = \mathbf{y}_1 + \mathbf{R}_2 \tag{13}$$

where $\mathbf{D}$ models an 8×8 block DCT, $\mathcal{Q}_2(\cdot)$ models quantization and dequantization processes with JPEG quantization table corresponding to a quality factor QF_2, and $\mathbf{E}_2$ is the error introduced by rounding and truncating the output values to eight bit integers. The last quantity $\mathbf{R}_2$ can be thought of as the overall error introduced by JPEG compression with respect to the original image.

Let us now suppose that the original image was previously JPEG compressed, starting from an uncompressed image $\mathbf{I_0}$, with a quality factor QF_1 and with a grid shifted by $(r, c) \neq (0, 0)$, $0 \leq r \leq 7$ and $0 \leq c \leq 7$, with respect to the upper left corner. This means that a generic 8×8 block chosen according to a grid aligned with the upper left corner will depend of four 8×8 blocks of the previously compressed image, i.e.,

$$\mathbf{y}_1 = \sum_{i=0}^{3} \mathbf{J}_{rc}^{(i)} \mathbf{y}_1^{(i)} \tag{14}$$

where $\mathbf{y}_1^{(i)}$, $i = 0, \ldots, 3$, denotes one of the four 8×8 blocks and $\mathbf{J}_{rc}^{(i)}$ models the shift between block $\mathbf{y}_1^{(i)}$ and block $\mathbf{y}_1$.

Each block $y_1^{(i)}$ is singly compressed, so according to (13) the image block $\mathbf{y}_2$ is doubly compressed and we can express it as

$$\mathbf{y}_2 = \sum_{i=0}^{3} \mathbf{J}_{rc}^{(i)} \left[\mathbf{D}^{-1}\mathcal{Q}_1(\mathbf{D}{\mathbf{I_0}}^{(i)}) + \mathbf{E}_1^{(i)}\right] + \mathbf{R}_2. \tag{15}$$

Let us assume that a block DCT with grid alignment (r, c) is applied to the doubly compressed image. In a similar way, we can model each 8×8 block as

$$\mathbf{y}_{2,rc} = \sum_{i=0}^{3} \tilde{\mathbf{J}}_{rc}^{(i)} \mathbf{y}_2^{(i)} \tag{16}$$

where $\mathbf{y}_2^{(i)}$, $i = 0, \ldots, 3$, denote four adjacent image blocks modeled as in (15) and $\tilde{\mathbf{J}}_{rc}^{(i)}$ model the reverse shift with respect to $\mathbf{J}_{rc}^{(i)}$. Since shifts and reverse shifts cancel each other, we can express the above image block as $\mathbf{y}_{2,rc} = \mathbf{D}^{-1}\mathcal{Q}_1(\mathbf{D}{\mathbf{I_0}}^{(0)}) + \mathbf{E}_1^{(0)} + \sum_{i=0}^{3} \tilde{\mathbf{J}}_{rc}^{(i)} \mathbf{R}_2^{(i)}$ and the corresponding DCT is given by

$$\mathbf{x} = \mathbf{D}\mathbf{y}_{2,rc} = \mathcal{Q}_1(\mathbf{D}{\mathbf{I_0}}^{(0)}) + \mathbf{D}\left(\mathbf{E}_1^{(0)} + \sum_{i=0}^{3} \tilde{\mathbf{J}}_{rc}^{(i)} \mathbf{R}_2^{(i)}\right). \tag{17}$$

By looking at the above equation, we can see that $\mathbf{x}$ is equal to a lattice point defined by the quantization $\mathcal{Q}_1()$ applied by the previous JPEG compression perturbed by a noise term due to the second JPEG compression and rounding/truncation errors. By invoking the central limit theorem, and neglecting truncation effects, we can assume the noise term approximately Gaussian and zero mean, so that the distribution of $\mathbf{x}$ can be modeled as in (2). Namely, the lattice generator matrix is diagonal and defined by

$$[\mathbf{\Theta}]_{ii} = Q_{1,i} \tag{18}$$

where $Q_{1,i}$ is the quantization step applied by the first JPEG compression on the ith DCT coefficients. As to the covariance matrix $\mathbf{C}$, this can be derived as

$$\mathbf{C} = \mathbf{D}\left(\mathbf{C}_{\mathbf{E}_1^{(0)}} + \sum_{i=0}^{3}\sum_{j=0}^{3} \tilde{\mathbf{J}}_{rc}^{(i)} \mathbf{C}_{\mathbf{R}_2}^{(ij)} \tilde{\mathbf{J}}_{rc}^{(j),T}\right)\mathbf{D}^T \tag{19}$$

where we assumed the independence of $\mathbf{E}_1^{(0)}$ and $\mathbf{R}_2^{(i)}$. By assuming the quantization errors independent and uniformly distributed in $(-0.5, 0.5)$, we have $\mathbf{C}_{\mathbf{E}_1^{(0)}} = \frac{1}{12}\mathbf{I}$. As to $\mathbf{C}_{\mathbf{R}_2}^{(ij)}$, from (13) we can express the approximation error as $\mathbf{R}_2 = \mathbf{D}^{-1}\left(\mathcal{Q}_2(\mathbf{D}\mathbf{y}_1) - \mathbf{D}\mathbf{y}_1\right)$. If we assume the quantization errors on DCT coefficients independent and uniformly distributed in $(-Q_2/2, Q_2/2)$, then we have $\mathbf{C}_{\mathbf{R}_2}^{(ij)} = \mathbf{0}$ when $i \neq j$ and we can express the covariance of $\mathbf{R}_2^{(i)}$ as

$$\mathbf{C}_{\mathbf{R}_2}^{(ii)} = \mathbf{D}^{-1}\mathbf{\Lambda}_{Q_2}\mathbf{D} \tag{20}$$

where $\mathbf{\Lambda}_{Q_2}$ is diagonal and $[\mathbf{\Lambda}_{Q_2}]_{ii} = Q_{2,i}^2/12$. Hence, the covariance matrix of the additive noise term is finally given as

$$\mathbf{C} = \mathbf{D}\left(\frac{1}{12}\mathbf{I} + \sum_{i=0}^{3} \tilde{\mathbf{J}}_{rc}^{(i)} \mathbf{D}^{-1}\mathbf{\Lambda}_{Q_2}\mathbf{D}\tilde{\mathbf{J}}_{rc}^{(i),T}\right)\mathbf{D}^T. \tag{21}$$

In the case of high frequency DCT coefficients, the hypothesis of uniformly distributed quantization errors usually does not hold. A possible correction is to modify $\mathbf{\Lambda}_{Q_2}$ by taking into account the average energy of the DCT coefficients at the different frequencies. In the following, we will use the approximation $[\mathbf{\Lambda}_{Q_2}]_{ii} = \max(Q_{2,i}^2/12, \sigma_{x,i}^2)$, where $\sigma_{x,i}^2$ denotes the variance of the ith DCT coefficient. It is worth noting that the above model can not be applied when $(r, c) = (0, 0)$, since the Gaussian approximation of the noise term in (17) does not hold.

B. Practical Detectors

The expressions derived in Section II, together with the $\mathbf{\Theta}$ and $\mathbf{C}$ estimated in the previous section, can be used to decide whether a single 8×8 JPEG image block has been singly

compressed or it has been previously compressed with a given quantization matrix $\mathcal{Q}_1$ and a given shift (r, c). However, in practice two problems have to be solved: i) the decision should be extended to the whole image; ii) both the quantization matrix of the previous compression and the grid shift are hidden parameters.

The optimal solution to the first problem would be to consider the joint distribution of the DCT coefficients on the whole image. Unfortunately, even for small images the above solution would soon become inpractical. A more practical solution is to assume that 8×8 blocks are independent, so that we can derive the likelihood ratio test as

$$\frac{p(\mathbf{x}|\mathcal{H}_1)}{p(\mathbf{x}|\mathcal{H}_0)} = \frac{\prod_k p(\mathbf{x}_k|\mathcal{H}_1)}{\prod_k p(\mathbf{x}_k|\mathcal{H}_0)} \tag{22}$$

where $\mathbf{x}_k$ denotes the DCT coefficients of the kth 8×8 block.

In order to solve the second problem, we can observe that it is a composite hypothesis testing problem where in the case of hypothesis $\mathcal{H}_1$ we have a collection of possible models indexed by parameters $\mathbf{\Theta}$ and $\mathbf{C}$. In this case, a possible solution is to use a generalized likelihood ratio test (GRLT), defined as

$$\frac{\max_{\mathbf{\Theta},\mathbf{C}} p(\mathbf{x}|\mathcal{H}_1; \mathbf{\Theta}, \mathbf{C})}{p(\mathbf{x}|\mathcal{H}_0)} \gtrless \tau. \tag{23}$$

Since the denominator in (23) does not depend on the hidden parameters, the GRLT can be expressed equivalently as

$$\max_{\mathbf{\Theta},\mathbf{C}} \mathcal{L}(\mathbf{x}; \mathbf{\Theta}, \mathbf{C}) \gtrless \tau. \tag{24}$$

IV. Experimental Results

A. Synthetic Signals

The proposed detectors have been first tested on synthetically generated signals. The signal $\mathbf{x}$ has been simulated as a vector of i.i.d. Gaussian variables with zero mean and variance $\sigma_x^2 = 1000$. Corresponding quantized versions have been obtained by quantizing the components of $\mathbf{x}$ according to the lattice defined as $[\mathbf{\Theta}]_{ii} = 2i/(N+1)$, $[\mathbf{\Theta}]_{ij} = 0,\ i \neq j$. The quantized versions have been perturbed by a Gaussian noise with AR(1) covariance structure, i.e., the covariance matrix can be expressed as

$$[\mathbf{C}]_{ij} = \frac{10^{-\mathrm{LNR}/10}}{12} \rho^{|i-j|} \tag{25}$$

where ρ is the correlation coefficient between adjacent components of $\mathbf{x}$. We considered ρ values ranging from 0 to 0.9, with step 0.1.

Tests have been performed on 10000 independently generated signals, with a number of dimensions N ranging from 2 to 20. Both the optimal and the separable detectors have been implemented by considering only the terms $\gamma(\mathbf{n}) \geq \epsilon$ in the expansion of (9) or $\exp(-2\pi^2 n_i^2/\psi_i) < \epsilon$ in the expansion of (10), where ϵ ranges from 1 to 10^{-3}.

In Fig. 1, we show the maximum accuracy achieved by the different detectors for different LNR values, for $N = 6$ and for $\rho = 0.2$ and $\rho = 0.7$. While for $\rho = 0.2$ all detectors achieve similar results, for $\rho = 0.7$ the optimal detector is clearly better than the others, whereas the distance detector appears greatly impaired.

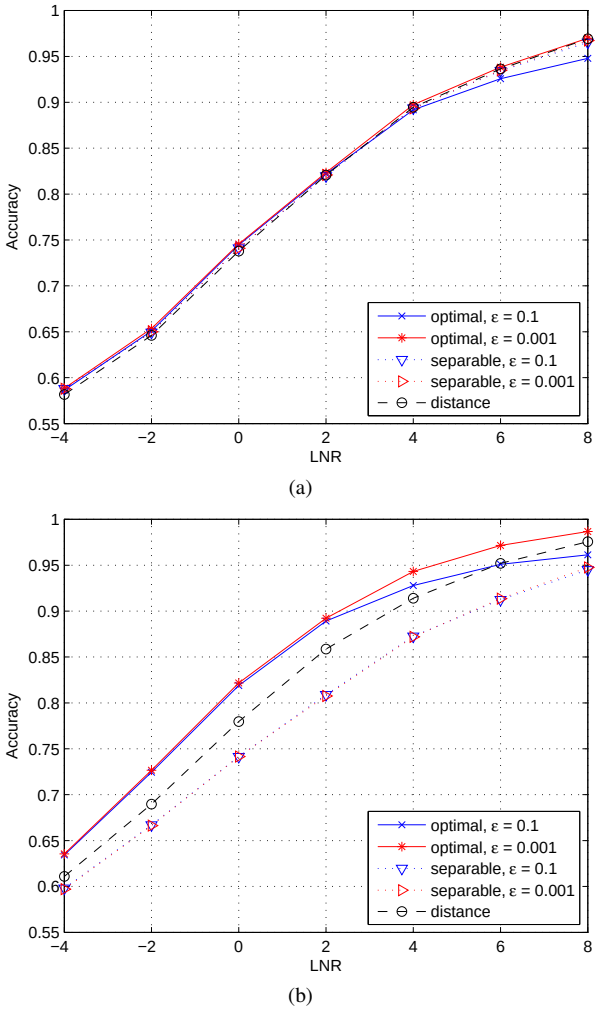

Fig. 1. Accuracy of the different detectors for $N = 6$: (a) $\rho = 0.2$; (b) $\rho = 0.7$.

In Fig. 2, we show the maximum accuracy achieved by the different detectors for different N and different ρ, for LNR = 0 dB. The optimal and separable detectors were computed using $\epsilon = 0.01$. We can observe that the optimal detector outperforms the other detectors for high ρ values. However, the performance of the optimal detector decreases with N. Preliminary results seem to show that in this configuration $\epsilon = 0.01$ is not enough to achieve a good approximation of $\mathcal{L}(\mathbf{x}; \mathbf{\Theta}, \mathbf{C})$. It is worth noting that it was not possible to compute the optimal detector for $\rho = 0.8$ and $N > 15$, due to the very large number of points in the Fourier expansion. Interestingly, in this scenario the separable detector does not appear very useful, since for low values of ρ and N all detectors have similar performance, whereas for high values of ρ and N the separable detector is definitely worse than the others.

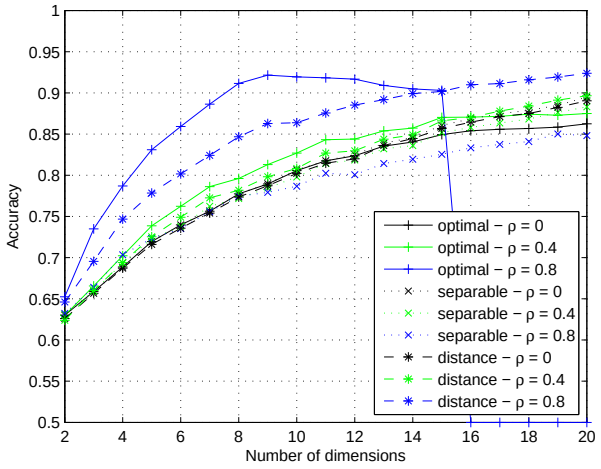

Fig. 2. Accuracy of the different detectors for LNR = 0 dB ($\epsilon = 0.01$).

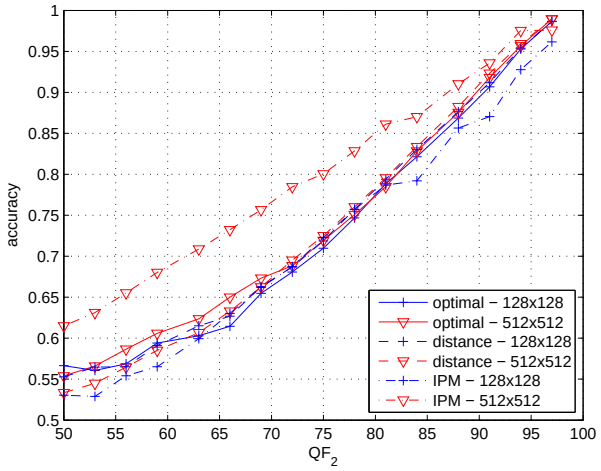

Fig. 3. Accuracy of the detectors for different JPEG qualities QF_2 and different image sizes.

B. JPEG Images

For the experimental validation on real images we used an image dataset composed by 1000 non-compressed TIFF images, having heterogeneous contents, coming from three different digital cameras and each acquired at its highest resolution; each test was performed by cropping the central portion using three different image sizes.

For simulating double JPEG compression, each original image was JPEG compressed with a quality factor QF_1, decompressed, cropped by a random shift $(r, c) \neq (0, 0)$, with $0 \leq r \leq 7$, $0 \leq c \leq 7$, and JPEG compressed with another quality factor QF_2. The absence of double compression was simulated by simply compressing the original image with a quality factor QF_2. The quality factor of both compressions was chosen so that the quantization step of the DC coefficients (Q_1) ranges from 1 to 16 with step 1.

The performance of the detector in (24) has been investigated by estimating the ROC curves for different combinations of (QF_1, QF_2), using a 5-fold cross validation strategy. Different optimal thresholds are chosen according to QF_2 and the image size. In a first experiment, the likelihood ratio in (24) is evaluated by taking the maximum over all the possible shifts $(r, c) \neq (0, 0)$ and all the possible QF_1. In a second experiment, the likelihood ratio in (24) is evaluated by taking the maximum over all the possible shifts $(r, c) \neq (0, 0)$ and all the possible $QF_1 \neq QF_2$. In all the above experiments, the detectors consider only the DC DCT coefficients for each 8×8 block, i.e., $N = 1$.

In Fig. 3, we show the maximum accuracy of the different detectors achieved in the first experiment for different values of QF_2 and different image sizes. The maximum accuracy is defined as the point on the ROC curve corresponding to the maximum number of correctly classified images and is averaged over all possible QF_1 values. For making comparisons, we report also the results obtained with the method of [9] based on integer periodicity maps (IPM). Surprisingly, in this scenario both the optimal and the distance detectors are

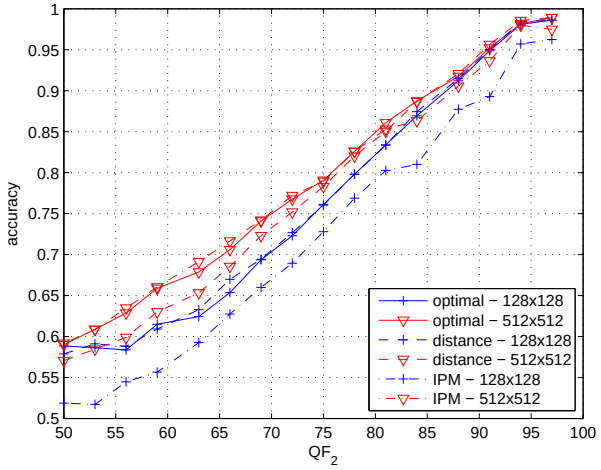

Fig. 4. Accuracy of the detectors for different JPEG qualities QF_2 and different image sizes, $QF_1 \neq QF_2$.

inferior to the IPM detector, which suggests that the model used in Section II has some problems with the non-aligned double JPEG scenario.

In Fig. 4, we show the maximum accuracy of the optimal and distance detectors achieved in the second experiment for different values of QF_2 and different image sizes. In this case, performances are evaluated for each configuration of QF_1, QF_2 such that $QF_1 \neq QF_2$. For making comparisons, we also report the results obtained with the method of [9] by excluding the case $QF_1 \neq QF_2$. Interestingly, in this case the performance of the optimal detector is better than that of the detector in [9], especially in the case of smaller images.

In Tables I and II we show the maximum accuracy of the optimal and distance detectors, respectively, for different combinations of QF_1 and QF_2, when the image size is 256×256. For a comparison, the accuracy of the detector in [9] is shown in Table III. In all tables, results are averaged only for configurations of QF_1, QF_2 such that $QF_1 \neq QF_2$. In this

TABLE I
ACCURACY OF THE OPTIMAL DETECTOR (%) FOR IMAGE SIZE 256×256, $QF_1 \neq QF_2$.

QF_1 \ QF_2	50-57	58-67	68-76	77-85	86-95	96
50-57	75.3	89.6	94.9	98.1	98.0	**99.6**
58-67	**64.9**	**84.0**	94.4	97.9	98.2	**96.8**
68-76	**52.8**	**61.3**	**82.2**	97.9	98.5	**99.6**
77-85	**52.0**	**50.5**	**52.9**	**76.8**	98.5	**98.8**
86-95	**52.2**	**50.9**	**50.1**	50.1	**74.9**	**99.8**

TABLE II
ACCURACY OF THE DISTANCE DETECTOR (%) FOR IMAGE SIZE 256×256, $QF_1 \neq QF_2$.

QF_1 \ QF_2	50-57	58-67	68-76	77-85	86-95	96
50-57	**78.1**	90.4	**95.5**	**98.5**	**98.5**	99.6
58-67	60.8	82.5	**95.2**	**98.5**	**98.6**	96.8
68-76	51.0	56.1	79.0	**98.5**	**98.9**	99.6
77-85	51.2	50.3	50.6	74.7	**98.8**	98.8
86-95	51.2	50.3	50.0	**50.2**	74.8	99.8

scenario, the optimal detector outperforms the detector in [9] for almost every configuration of QF_1, QF_2. It is interesting to note that the optimal detector has better performance when QF_1 and QF_2 are similar, whereas the distance detector has a slightly better performance when $QF_1 < QF_2$. This can be explained by noting that the latter case corresponds to a high LNR scenario, in which the distance detector is expected to achieve near optimal performance.

V. CONCLUSIONS

In this paper, we have derived an optimal detector for signals quantized on a given lattice under an infinite variance assumption and we have provided approximate expressions for its practical evaluation. Namely, for a low lattice-to-noise ratio (LNR) the optimal detector can be approximated by using a multidimensional Fourier expansion, whereas for a high LNR the optimal detector is almost equivalent to computing the distance from a lattice point. The proposed detector has been then applied to a practical image forensic problem, the detection of nonaligned double JPEG compression.

Results on synthetic signals show that the optimal detector achieves a significant advantage in the presence of correlated noise. However, this detector is not practical for a high number of dimensions, or for high LNR values, since the number of significant terms in the multidimensional Fourier expansion becomes very large. A simplified detector based on a separable Fourier expansion does not seem to provide significant advantages in the uncorrelated noise case, whereas it is clearly suboptimal in the correlated noise case.

TABLE III
ACCURACY OF THE DETECTOR IN [9] (%) FOR IMAGE SIZE 256×256, $QF_1 \neq QF_2$.

QF_1 \ QF_2	50-57	58-67	68-76	77-85	86-95	96
50-57	69.9	**92.0**	94.4	95.1	95.8	95.6
58-67	63.3	71.4	94.4	96.0	96.8	96.7
68-76	51.4	57.9	69.9	96.0	97.3	97.7
77-85	50.5	50.4	52.3	66.5	98.1	98.7
86-95	50.8	50.4	50.0	49.9	66.2	98.9

As to the detection of nonaligned double JPEG compression, the proposed model appears well suited as long as $QF_1 \neq QF_2$, in which case the optimal detector outperforms existing state-of-the art detectors. As to $QF_1 = QF_2$, a possible problem is that in this case DCT coefficients of singly compressed images are not uniformly distributed in a quantization bin, since the effects of the second quantization are visible also in the shifted DCT domain.

There are several avenues for further research. First of all, the proposed detector is optimal only when both $\boldsymbol{\Theta}$ and $\mathbf{C}$ are known. An interesting problem is whether the generalized likelihood ratio test may still have some optimality when such parameters are unknown, or alternative optimal tests exist. Then, there are some practical problems deserving further investigation, like how to cope with the case $QF_1 = QF_2$. Finally, the proposed approach can be applied also to solve different forensic problems, like the detection of a previous compression after geometric image manipulations.

ACKNOWLEDGMENT

This work was partially supported by the REWIND Project funded by the Future and Emerging Technologies (FET) programme within the 7FP of the European Commission, under FET-Open grant number: 268478.

REFERENCES

[1] H. Farid, "A survey of image forgery detection," *IEEE Signal Processing Mag.*, vol. 2, no. 26, pp. 16–25, 2009.
[2] Z. Fan and R. de Queiroz, "Identification of bitmap compression history: JPEG detection and quantizer estimation," *IEEE Transactions on Image Processing*, vol. 12, no. 2, pp. 230 – 235, Feb. 2003.
[3] H. Farid, "Exposing digital forgeries from JPEG ghosts," *IEEE Trans. Inf. Forensics Security*, vol. 4, no. 1, pp. 154–160, Mar. 2009.
[4] A. C. Popescu and H. Farid, "Statistical tools for digital forensics," in *In 6th International Workshop on Information Hiding*. Springer-Verlag, Berlin-Heidelberg, 2004, pp. 128–147.
[5] T. Bianchi and A. Piva, "Image forgery localization via block-grained analysis of JPEG artifacts," *IEEE Trans. Inf. Forensics Security*, vol. 7, no. 3, pp. 1003–1017, June 2012.
[6] D. Fu, Y. Q. Shi, and W. Su, "A generalized Benford's law for JPEG coefficients and its applications in image forensics," in *Proc. SPIE, Security, Steganography, and Watermarking of Multimedia Contents IX*, vol. 6505, San Jose, CA, USA, January 2007, pp. 1L1–1L11.
[7] S. Milani, M. Tagliasacchi, and S. Tubaro, "Discriminating multiple JPEG compression using first digit features," in *Proc. of ICASSP 2012*, Mar. 2012.
[8] W. Luo, Z. Qu, J. Huang, and G. Qui, "A novel method for detecting cropped and recompressed image block," in *Proc. of ICASSP 2007*, vol. 2, 2007, pp. II–217–II–220.
[9] T. Bianchi and A. Piva, "Detection of nonaligned double JPEG compression based on integer periodicity maps," *IEEE Trans. Inf. Forensics Security*, vol. 7, no. 2, Apr. 2012.
[10] ——, "Reverse engineering of double JPEG compression in the presence of image resizing," in *2012 IEEE International Workshop on Information Forensics and Security (WIFS)*, 2012, pp. 127–132.
[11] F. Pérez-González, F. Balado, and J. Martin, "Performance analysis of existing and new methods for data hiding with known-host information in additive channels," *IEEE Trans. Signal Process.*, vol. 51, no. 4, pp. 960 – 980, Apr. 2003.
[12] P. Vaidyanathan, *Multirate Systems And Filter Banks*, ser. Prentice Hall signal processing series. Pearson Education, 1993.